



Multiscale Methods in Beamed Energy Harnessing Applications

**BURT TILLEY
WORCESTER POLYTECHNIC INST MA**

**05/30/2019
Final Report**

DISTRIBUTION A: Distribution approved for public release.

**Air Force Research Laboratory
AF Office Of Scientific Research (AFOSR)/ RTB1
Arlington, Virginia 22203
Air Force Materiel Command**

DISTRIBUTION A: Distribution approved for public release.

REPORT DOCUMENTATION PAGE			<i>Form Approved</i> OMB No. 0704-0188		
<p>The public reporting burden for this collection of information is estimated to average 1 hour per response, including the time for reviewing instructions, searching existing data sources, gathering and maintaining the data needed, and completing and reviewing the collection of information. Send comments regarding this burden estimate or any other aspect of this collection of information, including suggestions for reducing the burden, to Department of Defense, Executive Services, Directorate (0704-0188). Respondents should be aware that notwithstanding any other provision of law, no person shall be subject to any penalty for failing to comply with a collection of information if it does not display a currently valid OMB control number.</p> <p>PLEASE DO NOT RETURN YOUR FORM TO THE ABOVE ORGANIZATION.</p>					
1. REPORT DATE (DD-MM-YYYY) 30-05-2019		2. REPORT TYPE Final Performance		3. DATES COVERED (From - To) 15 Sep 2015 to 14 Feb 2019	
4. TITLE AND SUBTITLE Multiscale Methods in Beamed Energy Harnessing Applications			5a. CONTRACT NUMBER		
			5b. GRANT NUMBER FA9550-15-1-0476		
			5c. PROGRAM ELEMENT NUMBER 61102F		
6. AUTHOR(S) BURT TILLEY, Rebecca Webb			5d. PROJECT NUMBER		
			5e. TASK NUMBER		
			5f. WORK UNIT NUMBER		
7. PERFORMING ORGANIZATION NAME(S) AND ADDRESS(ES) WORCESTER POLYTECHNIC INST MA 100 INSTITUTE RD WORCESTER, MA 01609-2280 US			8. PERFORMING ORGANIZATION REPORT NUMBER		
9. SPONSORING/MONITORING AGENCY NAME(S) AND ADDRESS(ES) AF Office of Scientific Research 875 N. Randolph St. Room 3112 Arlington, VA 22203			10. SPONSOR/MONITOR'S ACRONYM(S) AFRL/AFOSR RTB1		
			11. SPONSOR/MONITOR'S REPORT NUMBER(S) AFRL-AFOSR-VA-TR-2019-0141		
12. DISTRIBUTION/AVAILABILITY STATEMENT A DISTRIBUTION UNLIMITED: PB Public Release					
13. SUPPLEMENTARY NOTES					
14. ABSTRACT This research program centers on the fundamental heat-transfer processes for beamed-energy harnessing applications, such as electromagnetic heat exchangers. Of interest is to quantify the conversion efficiency of incoming electromagnetic radiation into elevated internal energy of a coolant. Electromagnetic-radiation absorbing materials, either porous or designed with channels through which a coolant can flow, that can withstand temperature up to 2000K, heat these materials through the application of electromagnetic waves. Coolant runs through the material to harness the desired energy. Since electrical conductivity of these materials depends on temperature, multiple steady temperatures are seen at the same input power. Asymptotic multiscale methods including homogenization are used to formulate an effective medium theory to describe the energy conservation and electric field amplitude propagation through this medium, for incompressible and compressible coolants. We find a resonance condition under which high temperatures can be achieved, but below the thermal and mechanical failure of the lossy medium for a thin laminated system.					
15. SUBJECT TERMS beamed energy, electromagnetic radiation, radiation absorbing, multiscale method, compressible coolant, incompressible coolant, finite-difference timedomain, microscale, macroscale					
16. SECURITY CLASSIFICATION OF:			17. LIMITATION OF ABSTRACT UU	18. NUMBER OF PAGES	19a. NAME OF RESPONSIBLE PERSON SAYIR, ALI
a. REPORT Unclassified	b. ABSTRACT Unclassified	c. THIS PAGE Unclassified			
Standard Form 298 (Rev. 8/98) Prescribed by ANSI Std. Z39.18					

DISTRIBUTION A: Distribution approved for public release.

				19b. TELEPHONE NUMBER <i>(Include area code)</i> 703-696-7236
--	--	--	--	---

AFOSR Final Performance Report

Project Title: Multiscale Methods in Beamed Energy Harnessing Applications

Award Number: FA9550-15-1-0476

Start Date: September 14, 2015

Program Manager: Dr. Ali Sayir
Air Force Office of Scientific Research
Aerospace Materials in Extreme Environments Program
875 North Randolph Street
Arlington, Virginia 22203-1768
E-mail: ali.sayir.2@us.af.mil
Phone: (703) 696-7236

Investigators: Prof. Burt S. Tilley (PI)
Prof. Vadim V. Yakovlev (Co-PI)
Department of Mathematical Sciences
Worcester Polytechnic Institute
100 Institute Road
Worcester, MA 01609
E-mail: tilley@wpi.edu
Phone: (508) 831-6664
Fax: (508) 831-5824

Abstract

This research program centers on the fundamental heat-transfer processes for beamed-energy harnessing applications, such as electromagnetic heat exchangers. Of interest is to quantify the conversion efficiency of incoming electromagnetic radiation into elevated internal energy of a coolant. Electromagnetic-radiation absorbing materials, either porous or designed with channels through which a coolant can flow, that can withstand temperature up to 2000 K, heat these materials through the application of electromagnetic waves. Coolant runs through the material to harness the desired energy. Since electrical conductivity of these materials depends on temperature, multiple steady temperatures are seen at the same input power. Asymptotic multiscale methods including homogenization are used to formulate an effective medium theory to describe the energy conservation and electric field amplitude propagation through this medium, for incompressible and compressible coolants. We find a resonance condition under which high temperatures can be achieved, but below the thermal and mechanical failure of the lossy medium for a thin laminated system. The analytical results for these laminated systems are compared favorably with direct numerical simulations. Extensions to porous media have been developed through homogenization methods, for both the classical and resonant (high-frequency) conditions. This latter work, along with a collaboration on electromagnetically-enhanced chemical vapor infiltration applications, is the focus of our ongoing work.

Keywords: Electromagnetic heating, computational methods, homogenization.

Accomplishments/New Findings

- In electromagnetic heat exchangers, electromagnetic energy is absorbed through a solid lossy dielectric. However, the loss factor of the ceramic depends on temperature, and hence the solution of the field strength and temperature must be done simultaneously. If a thin, lossy dielectric laminate is surrounded by two thin pure dielectric materials (either fluid or solid), electromagnetically resonant modes result in an additional branch to the power response curve. This new steady state can be utilized for energy harnessing, since the operating temperature is below the fracture temperature of the lossy material. In this case, spanwise conduction takes place much faster than streamwise conduction or convection.
- Streamwise energy transport limits the existence of this new steady-state solution near critical applied power levels.
- The transition between different steady states in this system is governed by a critical temperature. This result is supported through direct numerical simulations of a given set of physical materials.
- Preliminary results with gas coolants demonstrate that buoyancy forces can mitigate the appearance of the new resonant steady state.
- Effective model for electromagnetic wave propagation through spatially periodic composite material (composed of a pure dielectric and a lossy dielectric) has been derived when the spatial period of the geometry is comparable to the wavelength of the applied field. This model has been validated for laminated materials.
- Preliminary results show transients of the long-wave homogenization model can attain hot spots on the exterior of the sample prior to the onset of thermal runaway. This transient is driven by fluid flow through the medium carrying energy downstream to a locally insulated boundary.

1 Summary

A large number of space-based applications exist for the transmission of electromagnetic energy to a system some distance away. For example, work is being done to use a satellite to collect and convert solar energy into microwaves that will then be beamed to earth to help contribute to US energy production[1]. From the other direction, energy generated on earth could be transmitted to satellites to add to the power being generated by solar panels. Additionally, a ground-based infrared laser was used to power a UAV in early 2014 [2]. Along those lines, beamed energy propulsion has also been proposed as a method of improving current rocket propulsion capabilities[3]. A common thread in these technologies is the conversion of electromagnetic energy into a mechanically useful form.

The overall goal of this work is to determine the viability of a electromagnetic heat exchanger, where electromagnetic energy is harnessed as the power source by an absorbing material through which a coolant is heated, through computational and mathematical modeling. Unlike traditional microchannel heat exchangers [4, 5], a critical aspect of understanding this technology is the relation between the properties of an applied electromagnetic wave and the net transfer in internal energy of the coolant leaving the heat exchanger. This gain depends not only on the electric field amplitude, but also on the material properties of the heat exchanger, the heat exchanger's porous structure and the upstream applied flow rate of the coolant. To understand this relationship, models need to couple the electromagnetic heating of the heat exchanger, heat transfer from the exchanger to the coolant, and the flow of the coolant through the porous system from the physical fundamentals. Phenomenological relations are not appropriate in this modeling, since these expressions ignore the coupling between all of the different physical phenomena, and depend significantly on the experimental conditions.

In order for these applications to be feasible, the solid portion of the heat exchanger must be structurally stable at large temperatures (300 K to 2,000 K), and capable of absorbing a significant portion of the amplitude of the applied field. Ceramic materials such as silicon carbide and zirconia for example, are good candidates for this application, however, their electrical conductivity increases with temperature (see [6],[7] for two examples). Since the time-scale of the electromagnetic radiation is on the scale of nanoseconds, while thermal process evolve on a seconds time-scale, all of the modeling approaches prescribe the evolution of the electromagnetic electric field amplitude, at a prescribed carrier frequency, is quasi-steady on the time-scale of energy transfer.

Without any manner to remove the energy, temperature can grow in this model without bound, and this phenomenon is called *thermal runaway* in the microwave heating community. This phenomenon can be observed in processing applications, where the cavity shape can induce thermal runaway. The effect may occur regardless whether or not the sample is heated at a resonant or non-resonant frequency (Figure 1) or whether or not the loss factor is an increasing function of temperature (see [7]).

For sufficiently high conductivities, however, the electric field amplitude vanishes except near the boundary. A rapid loss in the field amplitude as it enters a new medium is called the *skin effect*, and this represents the conversion of the electromagnetic energy into internal energy. Power generation is limited to the boundary regions and the resulting average steady-state temperature in the medium is determined by the balance of net power in the boundary regions and energy losses to the environment.

To better understand the physical processes at work, consider a symmetric application of plane waves propagating normal to a uniform slab. Pelesko and Kriegsmann [6] observed that if traditional heat transfer is included in the model, then the temperature saturates when a balance of the net energy generated within the material by the applied field is balanced by energy losses to

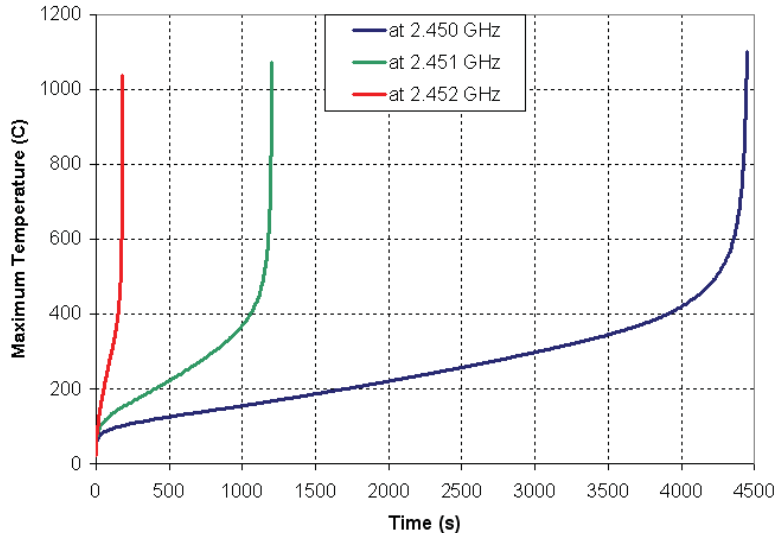


Figure 1: Example of time histories of maximum temperature in a cylindrical sample of zirconia microwave heated in a cavity at different (resonant, 2.452 GHz, and non-resonant, 2.451 and 2.45 GHz) frequencies (from [7])

the environment. A critical point in this balance is that a hysteresis is observed between the applied power and the temperature. At large temperatures, the electrical conductivity is large, and the field strength in the material is small, resulting in the power generation localized near the solid/environment boundary[8]. However, the temperatures of this upper branch are typically beyond the point where the mechanical and structural integrity of the material can be ensured.

The hysteresis behavior of these materials leads to some intriguing possibilities for energy transfer, provided that the lossy ceramic is not destroyed in the process. Once these materials are at sufficiently high temperatures, the amount of power needed to maintain this temperature is similar to the power needed to heat the material at a temperature along the lower branch. This suggests that if the material can be kept at higher temperatures, the energy transfer for a electromagnetically-driven heat exchanger might be quite efficient. However, the operating conditions of the exchanger can significantly affect the resulting hysteresis loop, since the upper branch is the result of the balance between the ohmic power in the energy equation and the net power removed from the material, including the power transferred to the fluid. A fundamental investigation on how these different physical processes interact is needed in order to determine the promise of this energy harnessing technique.

Microwave heating of laminated materials has additional complications to better understand the power absorption properties. In Kriegsmann and Tilley [9], a laminate structure of two solid material slabs, repeated periodically over space, is subject to a single applied plane wave whose incident wave vector direction is either perpendicular to the slab interfaces (the \mathcal{P} -problem), or tangent to these interfaces (the \mathcal{T} -problem). In the \mathcal{T} -problem, we can further consider two different polarizations: the TM -case, where the electric field is applied, or the TE -case, where the magnetic field is applied. The spatial period of these laminate pairs (called the *microscale*) is much smaller in practice than the characteristic length scale of interest (called the *macroscale*), and through an asymptotic approach known as homogenization, equations that represent the temperature and field strength are derived which depend on macroscale but include the net dominant physical effects occurring on the microscale. Through this analysis, in the \mathcal{T} -problem, significantly more power is

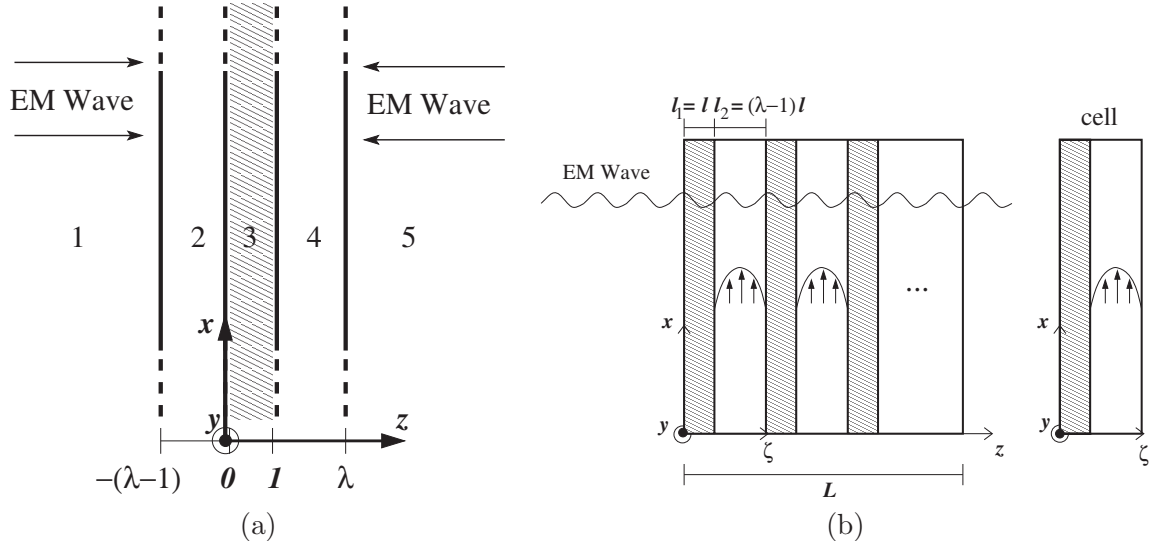


Figure 2: (a) Triple-layer laminate infinite strip domain. Regions 1 and 5 are free-space, regions 2 and 4 are a lossless dielectric, and region 3 is a lossy dielectric. Unit cell defined as two layers from $[0, \lambda]$. Symmetric monochromatic polarized plane waves impinge the external boundaries at normal incidence. (b) Configuration for development of effective medium theory for porous media. The widths λ in the figure are comparative to the wavelength of the applied electromagnetic radiation.

needed in the TE -polarization than the TM -polarization. However, the final steady-state thermal profile in the TE -polarization is elevated near the center of the material. Hence, in harnessing beamed energy, the orientation of the wave vector to the channels, and the polarization of the radiation can play a significant role in the effectiveness of the heat exchanger.

Effective models which capture the dominant physics in the microscale and their effect on macroscale dynamics are an attractive choice, since the mathematical description is computationally feasible, provides physical insight into the dominant macroscopic behaviors on the application time scales and operational frequencies, and their limits of validity are well understood[9, 10, 11]. Classical asymptotic approaches to these problems require the material to be spatially periodic at a fixed wavenumber[12, 13, 14]. However, materials that are influenced by many physical processes do not conform to this modeling paradigm.

Unlike the cases for microwave-frequency excitations described above, in the case of millimeter waves, the microscale solution to the electromagnetic-thermal problem can depend on the microscale. To understand the underlying phenomena that can be observed on the microscale, we considered the electromagnetic-thermal response of a lossy ceramic layer surrounded on either side by pure dielectrics. Figure 2a shows the configuration of interest. Plane waves are symmetrically applied to this three-layer laminate system, and energy losses to the environment (be they through advection or through radiation) are included. We found mathematical criteria on the geometry by which a third steady-state solution is achieved, provided that the energy losses to the environment are sufficiently small[15, 16, 17]. We confirmed this result through a series of COMSOL simulations[18]. Preliminary results are also describe for gaseous coolants and for porous pure-dielectric/lossy dielectric laminate systems.

The second vein of our work centers on effective media. Figure 2b shows the configuration of a series of alternating lossy ceramic layers (in grey) with pores in which contain a pure dielectric

incompressible fluid. Of interest is how the energy transfer from the electromagnetic radiation is absorbed in to the porous media. We formulated two systems of equations: long-wave homogenization system, for which the applied wavelength is much longer than the spatial periodicity of the geometry, and; high-frequency homogenization system, for which the applied wavelength is comparable to the spatial period of the geometry. For isothermal conditions, and for the geometry described in Figure 2b, the long-wave homogenization reduces to the classical mixture theory result, while the high-frequency homogenization recovers the results of the acoustic problem for loss-less materials[19]. Preliminary results are shown for the case of both models under an applied field with a prescribed fluid velocity.

An additional research collaboration with Prof. Jon Binner’s group at the University of Birmingham, UK. Mr. Matt Porter received funding from the J ECS Trust Collaboration Fellowship to visit WPI over the Spring 2018 semester. This work centered on microwave-enhanced chemical vapor infiltration (CVI) for fabricating silicon carbide parts from SiC fibrous preforms. Porter’s experimental work formed the basis for the modeling approaches used at WPI. One model centered on using FDTD methods, for non-reacting materials and ignoring convection effects within the material, to determine the power distribution profiles to be expected in the sample from the experimental configuration. The second model follows the reaction chemistry used in [8], but assuming that the reaction time scale is comparable to the thermal diffusion and advection time scales over the macroscale variables. Both preliminary results of the modeling approaches look promising.

2 High-Frequency Resonance in Triple-Layer Laminate Heat Exchangers

2.1 Overview

Consider the geometry shown in Figure 2a with plane waves symmetrically impinging the material from both sides at normal incidence. The electromagnetic waves, governed by Maxwell’s equations, propagate through the lossy material which generates heat. In this scenario, Maxwell’s equations are reduced to solving the one-dimensional Helmholtz equation in z . For a given constant temperature T , this field can be calculated analytically.

If we assume that energy losses to the environment are comparable to conduction in the three-layer laminate in the x -direction, then the temperature can be described as a function $T = T(x, t)$, independent of z to within the aspect ratio $\eta = \ell/L$. $T(x, t)$ evolves according to the following equation

$$\overline{\rho c_p} \frac{\partial T}{\partial t} = \overline{k} \frac{\partial^2 T}{\partial x^2} + P \sigma_3(T) \|E_3\|_2^2(T) - 2\mathcal{L}(T), \quad (1)$$

where $\overline{\rho c_p} = 1 + 2(\lambda - 1) \frac{K}{\alpha}$ is the effective heat capacity per unit volume, $\overline{k} = 1 + 2(\lambda - 1)K$ is an effective thermal conductivity, and $\mathcal{L}(T) = BiT + R[(T + 1)^4 - 1]$ is the external energy loss due to external convection and blackbody radiation respectively. The squared norm of the electric field is defined as $\|E_3\|_2^2 = \int |E_3|^2 dz$ and $|E_3|^2 = E_3 E_3^*$ where E_3^* is the complex conjugate of E_3 . The result of the thin domain assumption is that the evolution of temperature will depend only on time and on x .

2.2 Spatially-uniform steady-state solutions

Furthermore, if we assume that the electric field is uniformly applied along $-\infty < x < \infty$. This implies the diffusive thermal flux, $\overline{k} \frac{\partial T}{\partial x}$, is zero so the resulting equation governing the average temperature is

$$\frac{\partial T}{\partial t} = P \sigma_3(T) \|E_3\|_2^2(T) - 2\mathcal{L}(T), \quad (2)$$

We now define the *power response curve* as the bifurcation diagram of (P, T) , where T is the steady state temperature satisfying

$$P = \frac{2\mathcal{L}(T)}{\sigma_3(T) \|E_3\|_2^2(T)}. \quad (3)$$

Many dielectric materials have been empirically found to possess effective electric conductivities that exponentially increase in temperature, $\sigma_3 = A_3 e^{b_3 T}$. It is under this assumption that Kriegsmann et al. [20] found the power response curve defined as (3) to be S-shaped as shown in Figure 4a. It was later proven by Pelesko and Kriegsmann that the positively sloped branches of the power response curve are stable while the negatively sloped branch is unstable [6]. As power is increased past the lower branch, thermal runaway takes over and heats the material to the temperature at the upper branch. The only two stable states are for low temperatures, which is inefficient heating, and high temperatures, which may damage the material.

In our work, we require that the wavelength, permittivity, and layer width to satisfy the following: outer layer width is an odd multiple of a quarter wavelength $l(\lambda - 1) = (2m - 1) \frac{\lambda_2}{4}$ and the inner layer width is an odd multiple of a half wavelength $l = (2n - 1) \frac{\lambda_3}{2}$, where λ is the nondimensional width of a unit cell, where n, m are positive integers, and λ_j is the wavelength in region j . The unit cell defined by the domain $[0, \lambda]$. A commonly used term in homogenization theory it is comprised of the lossy layer and one of the lossless layers. These conditions are comparable to those for Bragg interference and Fabry-Pérot cavity, which establish a resonance and builds up the electric field inside the middle layer, as shown by Figure 3b. Additionally, it is a well known fact that this resonance is strengthened when there is high contrast between ϵ_2 and ϵ_3 . Figure 3a shows the electric field strength as ϵ_3 increases, thus increasing this contrast since $\epsilon_2 = \pi^2$. Resonance states show peaks in the electric field which increases as the contrast increases.

This change in the electric field transforms the S-shaped power response curve to a Double-S-shaped power response introducing two additional steady-state branches one of which is stable. Figure 4a depicts an S-curve while Figure 4b shows a Double-S-curve where the stable branches are plotted as solid lines and the unstable branches as dashed lines. The new stable branch occurs at the desired medium range temperatures for efficient heating while avoiding the damaging effects of thermal runaway. In addition, the power scale is reduced by two orders of magnitude. This allows us to use thermal runaway to our advantage. Increasing to a low power just past the first right turning point thermal runaway is induced, but comes to rest at a safe and efficient operating temperature on the middle branch.

The previous section reviews the existence of a Double-S-curve [15]. In this section, we consider the domain to be finite in the x -direction (vertically in Figure 2a), and relax the uniform heating assumption by applying a Dirichlet condition at one boundary and a zero flux condition at the

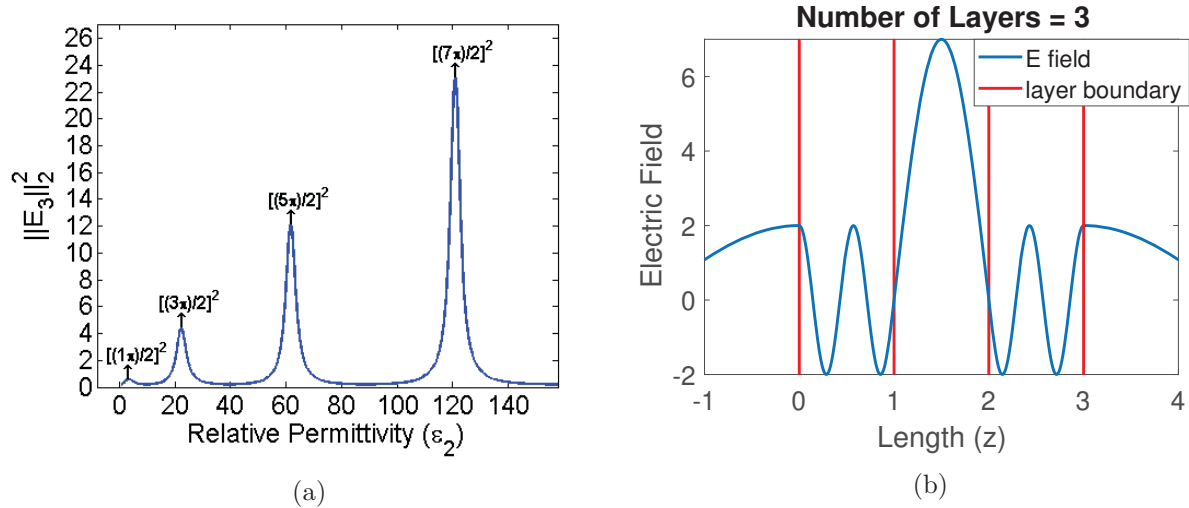


Figure 3: Electric field strength in middle lossy layer (region3) as a function of the outer layer permittivity. Peaks show Bragg resonance states with increasing field strength (a). Electric field (blue) within the triple-layer laminate boundaries (red) at a resonance state. Middle layer shows large electric field from applied resonance.

other. The governing equation is then given by (1) with boundary conditions),

$$T = 0, \quad x = 0, \quad (4)$$

$$\frac{\partial T}{\partial x} = 0, \quad x = L. \quad (5)$$

and a given initial condition. Physically, this models a thin three-layer laminate exposed to cold reservoir at $x = 0$ and sufficiently long enough for the material to heat up at the other boundary allowing the zero flux condition to be valid.

We are interested in how the power response curve changes as the diffusive transport change the heating effects. Figure 5a shows the power response for the uniform heating case while Figure 5b shows the power response curve when diffusive effects are considered. Increasing the thermal conductivity will produce regions where steady state solutions cease to exist. At these low power levels, the temperature will no longer have steady states and will decrease until it reaches a lower stable state. The existence boundaries were found analytically and were shown to agree with the computational results [17]. Similar results are found with this system for heat exchangers using incompressible coolants under laminar flow [16].

2.3 Direct Numerical Simulations

Direct computational simulations of this system for the full Helmholtz equation coupled to the energy equation, and subject to plane-wave radiation as described above were performed. COMSOL Multiphysics was used for the simulation, and the geometries used were consistent with plane waves in the microwave regime. The materials and geometry was chosen to be consistent with the resonant conditions where the double-S power response curve should appear. In Figure 6, we show how the results from the direct numerical simulation compares with the mathematical model for $Bi = 0.5, Bi = 0.25, Bi = 0.0625$. Radiation losses from the system were not incorporated in the model. We see that the COMSOL results agree quantitatively with the results from the

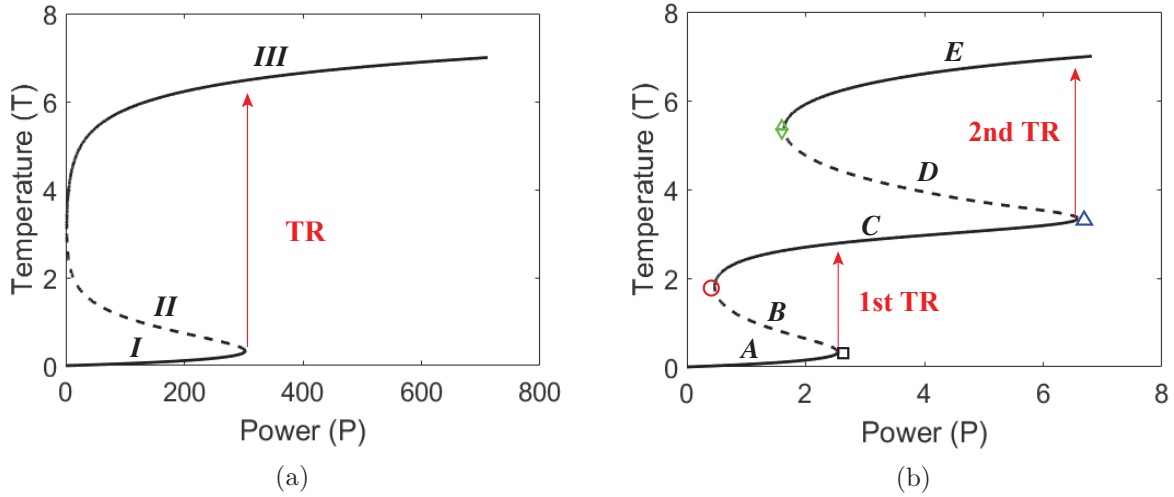


Figure 4: (left) Power response depicting S-curve where no resonance occurs for $\epsilon_2 = 9\pi^2$. The three branches are labeled with uppercase Roman numerals *I*, *II*, *III*. The red arrow labeled 'TR' indicates the thermal runaway event. (right) Power response depicting Double-S-curve where resonance is established for $\epsilon_2 = (\frac{7\pi}{2})^2$. The five branches are labeled with uppercase letters *A*, *B*, *C*, *D*, *E* and the four turning points are labeled first through fourth with colored symbols \square , \circ , \triangle , and \diamond respectively. The two red arrows labeled 'TR' indicate the two separate thermal runaway events. Additional parameters for both graphs include $\epsilon_m = \pi^2$, $K = 0.5$, $Bi = 0.5$, $Q = 0$, $\sigma_3(T) = 10^{-3}e^{3T}$

mathematical model described above in the limit when heat losses to the environment are small. In this limit, the temperature within the system is uniform in the spanwise direction.

Although the power level at which thermal runaway takes place between the two models can vary significantly based on Bi , the temperature at which this transition takes place is nearly consistent for all Bi considered. We hypothesize that the system has a critical temperature at which the thermal runaway event is triggered.

2.4 Ongoing Work

2.4.1 Gas Coolants

The operating temperatures of these heat exchangers are expected to be on the order of 1000 K. Under these conditions, coolants are necessarily going to be gaseous. Currently, we are focusing on how buoyancy effects in a gaseous coolant affects the thermal runaway transition found in the lossy dielectric laminate. To consider this case, we consider the lossless dielectrics to be an ideal gas, and the channels are now sealed on each end to ensure that the net mass flow in the gas is zero. We note that the dielectric constant in the gas is a function of the gas density, so we set the ambient pressure in each chamber so that the high-frequency resonance is expected to take place.

Buoyancy plays a very important role in the behavior of this system. In Figure 7, gravity is acting in the negative Y direction, and we show the temperature, velocity amplitude, and pressure within the gas chamber when the applied power is $P_{in} = 5, 100 \text{ W/m}^2$ (left) and $P_{in} = 5, 200 \text{ W/m}^2$ (right). Note that this relatively small increment in the applied power leads to thermal runaway within the lossy dielectric, and a convection roll is set up within the gas. Gas is driven by buoyancy vertically along the Gauss/ceramic boundary, and a return flow is driven along the gas/external

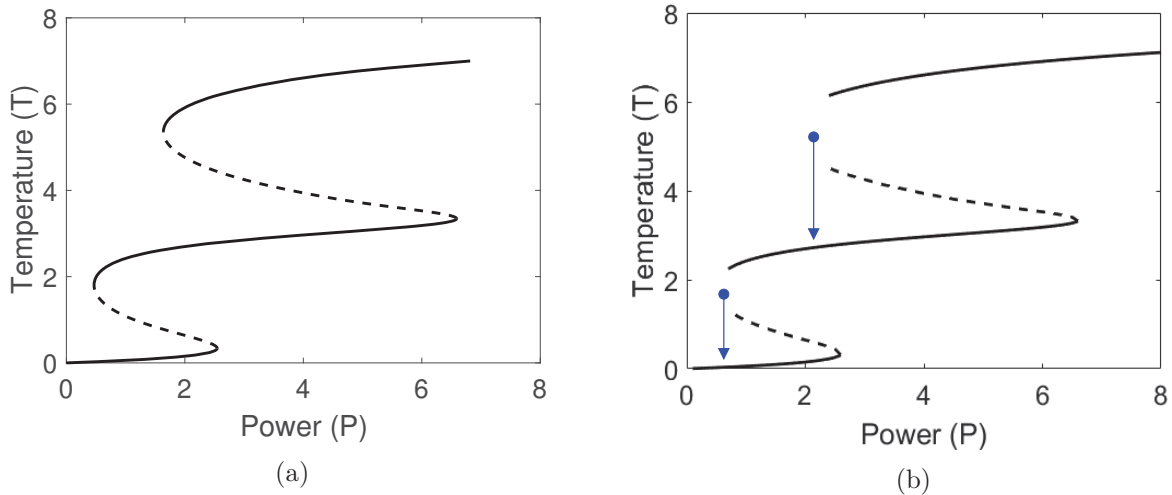


Figure 5: Power response of (2) for uniform heating in x (a), power response of (1) for nonuniform heating in x with $\bar{k} = 0.5$. Nonexistence regions where steady states cease appear near the left two turning points. Blue arrows show how temperature decreases within the nonexistence regions (b). Other parameters used to produce these curves include $\epsilon_f = \left(\frac{7\pi}{2}\right)^2$, $\epsilon_m = \pi^2$, $\gamma = 1$, $K = 0.5$, $Bi = 0.5$, $Q = 0$, $\sigma_3(T) = 10^{-3}e^{3T}$

boundary. Pressure here reflects primarily the density stratification which is driven by the thermal gradients within the ceramic.

When the system orientation is rotated so that gravity is now acting along the positive X -direction, we see that buoyancy significantly affects the thermal behavior of the system. In Figure 8, we consider the cases when $P_{in} = 5,100\text{W/m}^2$ (left), and $P_{in} = 6,000\text{W/m}^2$ (right). Notice that at these applied power levels, Rayleigh-Bénard convection rolls have developed within the gas layer, with the spatial period is governed by the spanwise thickness of the gas chamber. These convection rolls significantly enhance thermal transport from the ceramic, to the point when the thermal runaway transition is quenched. Further study in this area focuses on how the orientation of the system affects the transition.

2.4.2 Porous Lossless Laminates

As described above, the gas pressure can be adjusted initially to vary the permittivity. However, the practicality of this affect is very limited, and we have begun to determine the possibility of using lossless porous materials in the pure dielectric region shown in Figure 2a. The benefit of this method is that we can use mixture theory in this region, since the wavelength of the field, for the resonance conditions within the heat exchanger, are long compared to the pore scale. Preliminary results suggest that the increase in the applied pressure drop which drives the incompressible fluid flow can act to quench the thermal runaway transition. The mechanisms of this quenching are not completely understood at this writing, but will be a current effort in the coming year.

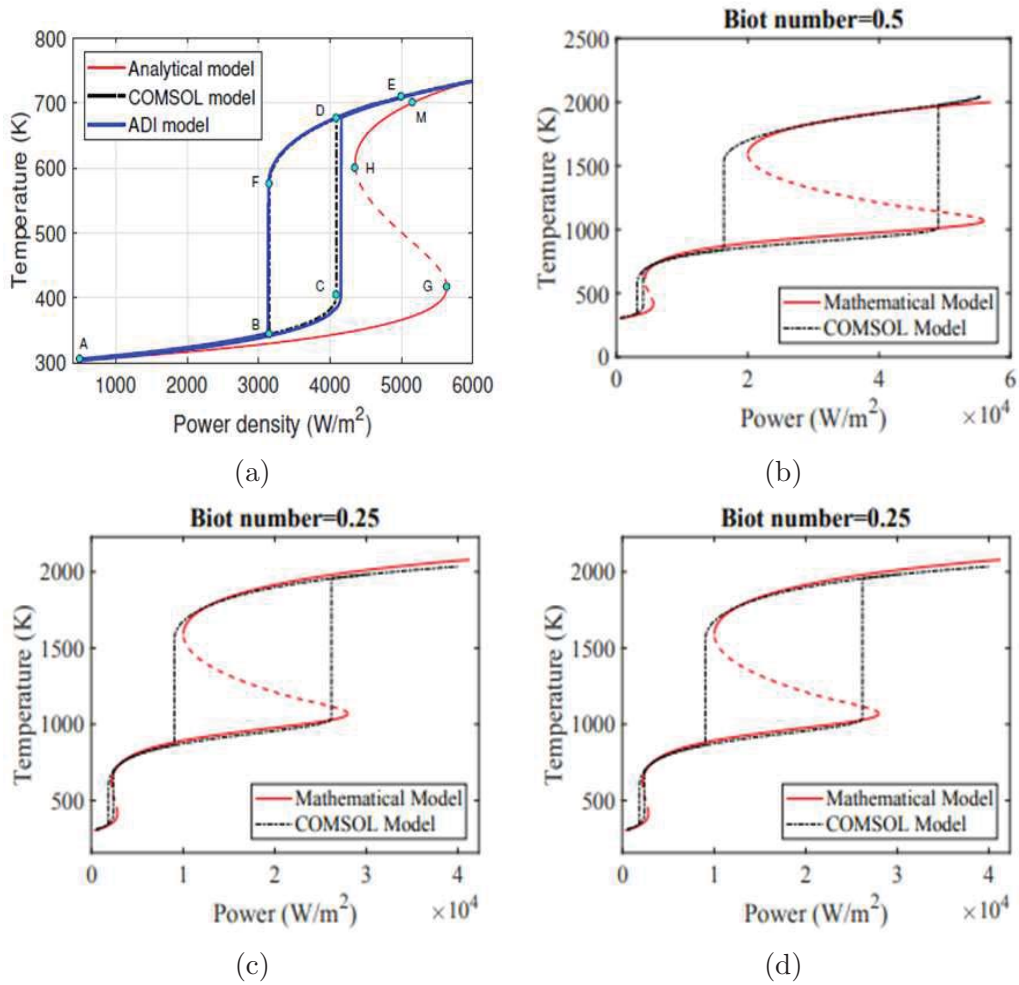


Figure 6: Comparison of the power response curves generated by the mathematical model under resonant conditions, and a direct numerical simulation using COMSOL for a variety of Biot numbers Bi . [21]

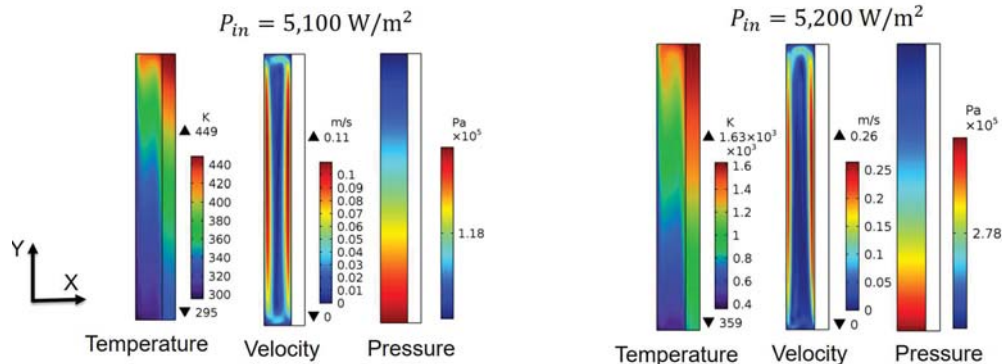


Figure 7: Gas and thermal steady state for a symmetric system with a dielectric gas in a closed cavity next to an electromagnetically lossy layer. Gravity is acting in the negative vertical direction. Left: Lower temperature solution of power response curve. Right: Larger temperature solution corresponding to the power response curve. Note the the transition between these states is over a small change in the applied power.

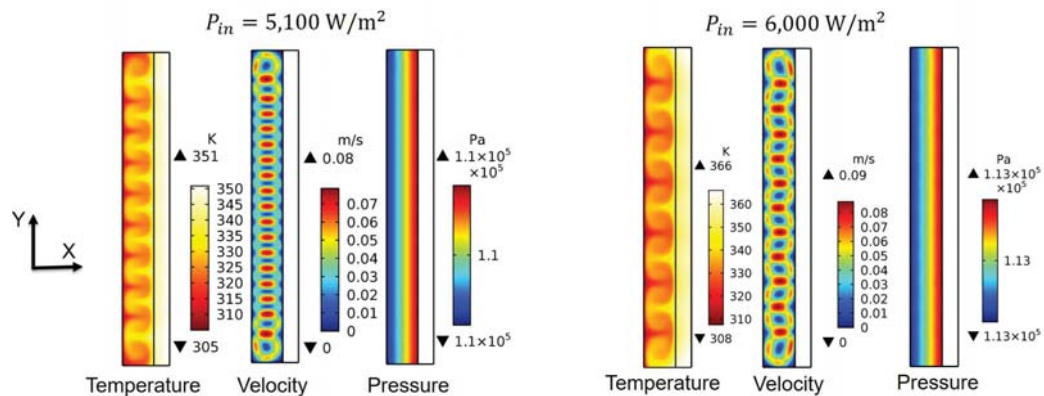


Figure 8: Gas and thermal steady state for a symmetric system with a dielectric gas in a closed cavity next to an electromagnetically lossy layer. Gravity is acting in the positive horizontal direction. Left: Lower temperature solution of power response curve. Right: Similar temperature solution corresponding to the power response curve. Note the the transition between these states is over a small change in the applied power. Note that the development of convection roles improves gas transfer from the lossy material, preventing thermal runaway.

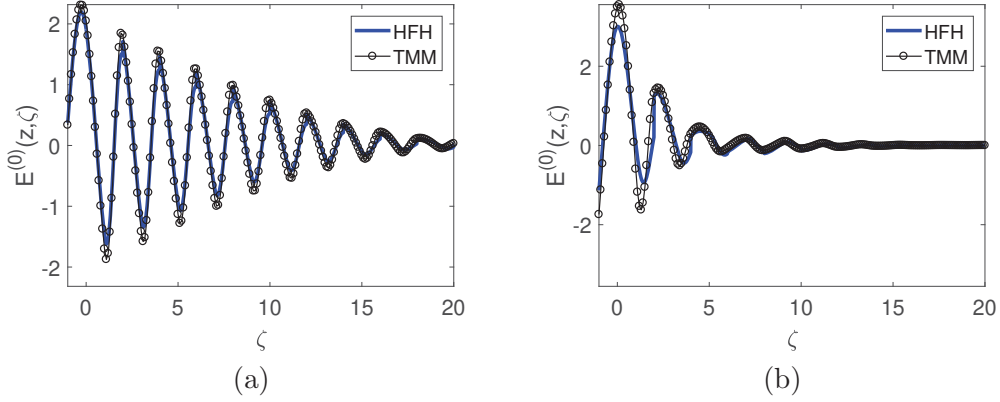


Figure 9: Comparison of High-frequency Homogenization solutions to those of the Transfer Matrix Method (a) $N = 50$, $\epsilon'' = 0.1$ (b), $N = 50$, $\epsilon'' = 1$.

3 High-Frequency Homogenization of Maxwells Equations for Low-loss Porous Dielectrics

Consider the configuration shown in Figure 2b. An electric field, polarized normal to the plane, is propagating through a laminate structure with a lossy ceramic (gray) and an incompressible pure dielectric fluid (white). The cases investigated with this award centers on laminar flows within the liquid. We apply homogenization techniques to this system to find effective equations that govern the temperature and the electric field within the composite medium.

In this work, we assumed that the power coefficient P in Equation (1) was small enough (or the loss factor of the ceramic is small enough) so that a uniform temperature over the microscale is an appropriate approximation. With this assumption, classical homogenization approaches lead to the following energy equation over the macroscale variables (z, x, t)

$$\frac{\partial T}{\partial t} + \alpha Pe \bar{u} \frac{\partial T}{\partial x} = \nabla (\mathbf{A} \nabla T) + P \sigma_3(T) \|\mathbf{E}\|_2^2(T), \quad (6)$$

where α is the thermal diffusivity ratio, Pe is the Péclet number, \bar{u} is the average fluid velocity, \mathbf{A} is a thermal diffusivity tensor, which depends on the microscale geometry. This nonlinear equation for the temperature depends on the behavior of the electric field \mathbf{E} within the medium, which itself depends on temperature.

For the effective equation for the electric field, we pursued two different limits. The first, and a classical results[9, 22], focused on the case when the wavelength of the electric field is much longer than the characteristic microscale length (λ in Figure 2b). The second approach, which is a modification of the high-frequency homogenization approach by Craster et al.[19], we derived a general amplitude equation of a single mode on a triply-periodic composite microscale pattern. Figure 9 shows a comparison of our model for the geometry shown in Figure 2b to the exact solution found using the Transfer Matrix Method. The agreement is excellent. Our method captures the loss of the band gap in these structures when any dissipation is included [16].

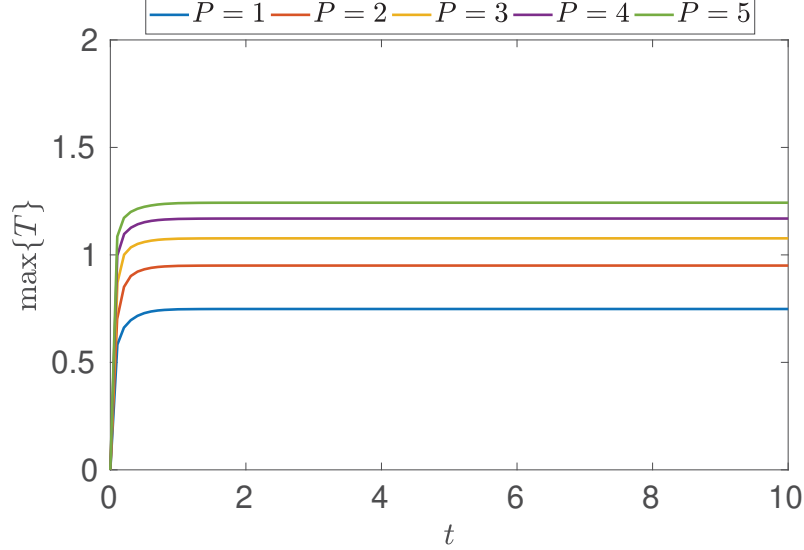


Figure 10: Maximum temperature T within an effective porous medium with $\alpha = 2$, $Pe = 1$, plane wave excitation along $z = 0$, and normal gradients zero along the other boundaries. Note that the maximum temperature in this case increases monotonically, but with smaller changes in magnitude, as the applied power P is increased.

3.1 Ongoing Work

3.1.1 Long-Wave Excitations

We have developed a computational implementation of the long-wave homogenization model in [16]. This implementation solves the energy equation (6) subject to the long-wave homogenization approach found in Wellander and Kristensson [22]. We have a sample on a unit square $0 < x, z < 1$ of a porous material in the structure of Figure 2b, with fluid entering the domain at $x = 0$, and a plane wave exiting the medium along $z = 0$. We assume that normal derivatives of the field and the temperature are zero along the other boundaries, with the exception of Newton’s law of cooling along $z = 0$, and symmetry conditions along $z = 1$.

Figure 10 shows the transient of the maximum temperature in the medium over time for several different power levels. We note that each transient reaches a stable temperature profile quickly in time, and that the increase in this maximum equilibrium temperature per change in the applied power is reduced as P is increased. The physical mechanisms for this change can be observed in Figure 11. Here, we show the steady-state profiles for $|\mathbf{E}|$ (a) and temperature T (b) for $P = 1$, while (c) shows the field strength $|\mathbf{E}|$ and (d) the temperature for and $P = 5$. For $P = 1$, the skin depth is nearly the full length of the sample, which leads to classical volumetric heating. The presence of the fluid flow from the bottom to the top carries energy near the corner $(z, x) = (1, 1)$. The high temperature leads to a slightly reduces skin depth in the upper half of the sample.

For $P = 5$, the physical mechanisms are significantly different. In this case, the skin depth is significantly smaller than the case for $P = 1$. Hence, the majority of the power is generated along $z = 0$, and fluid advection carries this energy local to the corner $(z, x) = (0, 1)$. Localized heating in this region is mitigated by Newton’s law of cooling along $z = 0$ and the advection carrying relatively cooler fluid along $z = 1$ through the sample. These two mechanisms limit the growth of the hot spot within the skin layer.

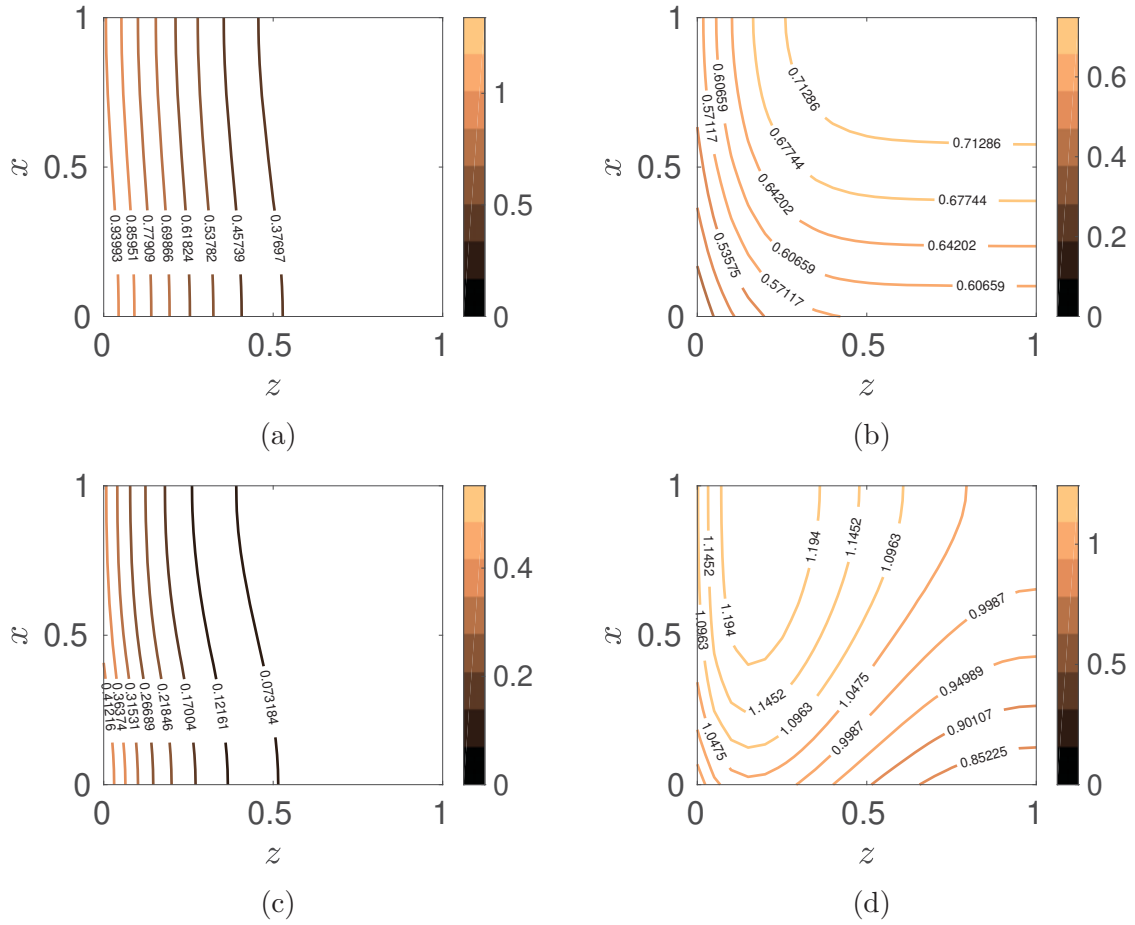


Figure 11: Examples of the long-wave homogenization response for a material with $\alpha = 2$, $B = 2$, and $Pe = 1$. (a) $|\mathbf{E}|$ for $P = 1$ at $t = 10$. (b) $T(z, x, 10)$ with $P = 1$. (c) $|\mathbf{E}|$ for $P = 5$ at $t = 10$. (d) $T(z, x, 10)$ with $P = 5$. Note that the hot spot remains within the skin layer of the electric field.

3.1.2 High-Frequency Excitation

We are developing a computational implementation of the high-frequency homogenization model found in Gaone (2018)[16]. We shall follow with the same macroscale parameter choices as is found in the long-wave homogenization section above. This direct comparison will consider the different energy absorption and transport under different two-dimensional spatially-periodic modes on the microscale. This work will be submitted for peer-review by the end of Summer 2019.

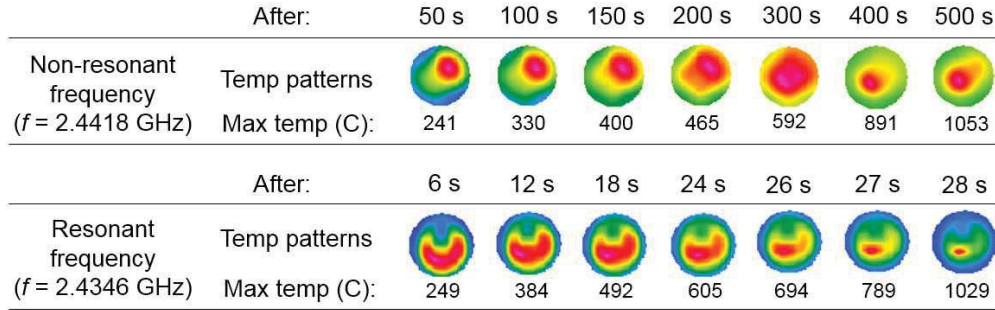


Figure 12: Non-normalized patterns of temperature evolution in the central plane through a 55×8 mm disk of stacked SiC fabric plies heated in SAIREM Labotron (power 1.1 kW).

4 Ongoing Collaboration with Dr. Jon Binner, University of Birmingham, UK

The ongoing cooperation with Prof. Binner's group in the School of Metallurgy and Materials, University of Birmingham, U.K., is focused on computational study of microwave thermal processing of SiC fabric. The objective is to clarify electromagnetic and thermal processes occurring in the course of microwave-enhanced chemical vapor infiltration (CVI). The CVI is a process in which a solid matrix is deposited into a porous preform by the thermal decomposition of a reactive gaseous mixture. Difficulties to control microwave processing of the material demand development and exploitation of a numerical model capable of simulating microwave-induced temperature field in the material heated in a high power microwave reactor. Initial computational results are informative and instructive. Figure 12 shows that when the processed SiC disk is heated at a non-resonant cavity frequency, due to low energy coupling, the heating rate is relatively slow, and sufficient uniformity of heating is supported by thermal conductivity of the material. In contrast, at a resonant cavity frequency, thermal runaway occurs: after reaching 605 C for the first 24 s, maximum temperature increases by 425 C for the last 4 s. Moreover, the heating is characterized by development of a strong hot spot potentially damaging to the sample. Additionally, a second long-wave homogenization model is being developed which incorporates the reaction chemistry and the dynamic change of the evolving pore structure and the resulting energy, species, and gas transport.

References

- [1] K. Lee. NASA Wants to Beam Microwave Energy to Earth with a Solar Power Plant in Space. <http://inhabitat.com/nasa-wants-to-beam-microwave-energy-to-earth-with-a-solar-power-plant-in-space/>. Accessed: 17-Feb-2015.
- [2] NASA Armstrong Fact Sheet: Beamed Laser Power for UAVs. <http://www.nasa.gov/centers/armstrong/news/FactSheets/FS-087-DFRC.html>. Accessed: 17-Feb-2015.
- [3] K.L.G. Parkin, L.D. DiDomenico, and F.E.C. Culick. The Microwave Thermal Thruster Concept. In K. Komurasaki, editor, *Beamed Energy Propulsion: Second International Symposium on Beamed Energy Propulsion*, pages 418–429. Amer. Inst. Phys., 2004.
- [4] D.B. Tuckerman and R.F.W. Pease. High-Performance Heat Sinking for VLSI. *IEEE Elec. Dev. Letters*, EDL-2(5), 1981.
- [5] J. Goodling. Microchannel heat exchangers - a review. In *High Heat Flux Engineering II, Proc. of SPIE 1993*, 1997.
- [6] J.A. Pelesko and G.A. Kriegsmann. Microwave heating of ceramic laminates. *J. Eng. Math.*, 32:1–18, 1997.
- [7] V.V. Yakovlev, S.M. Allan, M.L. Fall, and H.S. Shulman. Computational Study of Thermal Runaway in Microwave Processing of Zirconia. In J. Tao, editor, *Microwave and RF Power Applications*, page 303:306. Cépaduès Éditions, 2011.
- [8] B.S. Tilley and G.A. Kriegsmann. Microwave-enhanced chemical vapor infiltration: a sharp interface model. *J. Eng. Math*, 41:33, 2001.
- [9] G.A. Kriegsmann and B.S. Tilley. Microwave heating of laminate panels. *J. Eng. Math.*, 44:173, 2002.
- [10] T.M. Segin, L. Kondic, and B.S. Tilley. Long-wave linear stability theory of a compressible gas-liquid two-layer flow system. *IMA J. Appl. Math.*, 71:715–739, 2006.
- [11] B.D. Storey, B.S. Tilley, H. Lin, and J.G. Santiago. Electrokinetic instabilities in thin microchannels. *Phys. Fluids*, 17(1):018103, 2005.
- [12] K. Terzaghi and R.B. Peck. *Soil Mechanics for Unsaturated Soils*. John Wiley & Sons, 1948.
- [13] H.I. Ene and D. Polisevski. *Thermal Flow in Porous Media*. D. Reidel Publishing, 1987.
- [14] C.C. Mei and B. Vernescu. *Homogenization Methods for Multiscale Mechanics*. World Scientific, 2011.
- [15] J.M. Gaone, B.S. Tilley, and V.V. Yakovlev. Permittivity-based control of thermal runaway in a triple-layer laminate. In *IEEE MTT-S Intern. Microwave Symp. Dig.*, (Honolulu, HI, June 2017), 978-1-5090-6360-4.
- [16] J.M. Gaone. *An Asymptotic Approach to Modeling Wave-Geometry Interactions in an Electromagnetic Heat Exchanger*. PhD thesis, Worcester Polytechnic Institute, 2018.

- [17] J.M. Gaone, B.S. Tilley, and V.V. Yakovlev. Electromagnetic heating control via high-frequency resonance of a triple-layer laminate. *J. Eng. Math.*, 114(1):65–86, 2019.
- [18] A.A. Mohekar, J.M. Gaone, B.S. Tilley, and V.V. Yakovelev. Multiphysics simulation of temperature profiles in a triple-layer model of a microwave heat exchanger. In *IEEE MTT-S Intern. Microwave Symp. Dig.*, pages 1389–1392, (Philadelphia, PA, June 2018) 978-1-5386-5067-7.
- [19] R.V. Craster, J. Kaplunov, and A.V. Pichugin. High-frequency homogenization for periodic media. *Proc. R. Soc. A*, 466:23412362, 2010.
- [20] G.A. Kriegsmann, M.E. Brodwin, and D.G. Watters. Microwave heating of a ceramic halfspace. *SIAM J. Appl. Math.*, 50(4):1088–1098, 1990.
- [21] A.A. Mohekar. Computational modeling of triple layered microwave heat exchangers. Master’s thesis, Worcester Polytechnic Institute, 2018.
- [22] N. Wellander and G. Kristensson. Homogenization of the Maxwell Equations at Fixed Frequency. *SIAM J. on Appl. Math.*, 64(1):170–195, 2003.

Personnel:

Faculty: Prof. B.S. Tilley (WPI)
Prof. V.V. Yakovlev (WPI)

Graduate Student: Dr. Joseph M. Gaone (WPI), 2015-2018
Mr. Ajit Mohekar (WPI), 2017-2018.
Mr. Matt M. Porter (Univ. Birmingham). Spring 2018.
(Funded through a JECS Trust Collaboration Fellowship)

Undergraduate Student: Ms. Darien Gaudet, Summer 2018.

Collaborator: Dr. Brad Hoff, AFRL-Kirtland

Publications

1. J. M.Gaone, B. S. Tilley, V. V. Yakovlev, Permittivity-Based Control of Thermal Runaway in a Triple-Layer Laminate, *2017 IEEE MTT-S International Microwave Symposium*, June 2017. 978-1-5090-6360-4
2. A.A. Mohekar, J.M. Gaone, V.V. Yakovlev, B.S. Tilley, A 2D-Coupled Electromagnetic, Thermal and Fluid Flow Model: Application to Layered Microwave Heat Exchangers, *2018 IEEE MTT-S International Microwave Symposium*, June 2018, pp. 1389-1392.
3. A.A. Mohekar, J.M. Gaone, B.S. Tilley, and V.V. Yakovlev, Multiphysics simulation of temperature profiles in a triple-layer model of a microwave heat exchanger, *IMPIs 52nd Annual Microwave Power Symposium*, June 2018, pp. 33-35.
4. J.M. Gaone, B.S. Tilley, V.V. Yakovlev, Electromagnetic Control by High-Frequency Resonance of a Triple-Layer Laminate, *J. Eng. Math*, **114**(1), 65-86: 2019.
5. J.M. Gaone, B.S. Tilley, V.V. Yakovlev, Asymptotic Modeling of High-Frequency Electromagnetic Heating of Triple-Layer Heat Exchanger, *SIAM J. Applied Math.*, in preparation. Submission expected August 2019.
6. A.A. Mohekar, J.M. Gaone, V.V. Yakovlev, and B.S. Tilley, A 2D Numerical Model of a Triple-Layer Electromagnetic Heat Exchanger, *IEEE J. on Multiscale and Multiphysics Comp. Tech.*, Submission expected July 2019.
7. J.M. Gaone, B.S. Tilley, V.V. Yakovlev, High-Frequency Homogenization of Maxwells Equations for Low-loss Porous Dielectrics, *Math. Methods in Appl. Sci.*, in preparation. Submission expected August 2019.
8. J.M. Gaone, An Asymptotic Approach to Modeling Wave-Geometry Interactions in an Electromagnetic Heat Exchanger, PhD Thesis, Mathematical Sciences, Worcester Polytechnic Institute, May 2018
9. A.A. Mohekar, Computational Modeling of Triple Layered Microwave Heat Exchangers, MS Thesis, Mechanical Engineering, Worcester Polytechnic Institute, May 2018.
10. A.A. Mohekar, B.S. Tilley, V.V. Yakovlev, A 2D Model of a Triple Layer Electromagnetic Heat Exchanger with Porous Media Flow, *2019 IEEE MTT-S International Microwave Symposium*, Boston, MA, June 2019 (accepted).

11. A.A. Mohekar, B.S. Tilley, V.V. Yakovlev, Plane Wave Irradiation of a Layered System: Resonance-Based Control over Thermal Runaway, *17th Intern. Conference on Microwave and High Frequency Heating (AMPERE 2019)*, Valencia, Spain, September 2019 (accepted).

Interactions/Transitions:

1. J.M.Gaone, B.S. Tilley, V.V. Yakovlev, Permittivity-Based Control of Thermal Runaway in a Triple-Layer Laminate, Graduate Research Innovation Exchange (Finalist), Worcester Polytechnic Institute, Worcester MA, February (April), 2017 (poster)
2. J.M.Gaone, B.S. Tilley, V.V. Yakovlev, Permittivity-Based Control of Thermal Runaway in a Triple-Layer Laminate, Mathematical Modeling Group, Worcester Polytechnic Institute, Worcester MA, March 2017.
3. J.M.Gaone, B.S. Tilley, V.V. Yakovlev, Permittivity-Based Control of Thermal Runaway in a Triple-Layer Laminate, *Applied Math Days*, Rensselaer Polytechnic Institute, Troy NY, April 2017
4. J.M.Gaone, B.S. Tilley, V.V. Yakovlev, Permittivity-Based Control of Thermal Runaway in a Triple-Layer Laminate, *2017 IEEE MTT-S International Microwave Symposium*, Honolulu HI, June 2017.
5. J.M.Gaone, B.S. Tilley, V.V. Yakovlev, Microwave Heating: From Defrosting Steak to Turning Turbines, *2017 IEEE MTT-S International Microwave Symposium: 3 Minute Thesis*, Honolulu HI, June 2017.
6. J.M.Gaone, B.S. Tilley, V.V. Yakovlev, A Mathematical Model of Microwave Heating a Dielectric Layer for Channel Flow Energy Collection, *Society for Industrial and Applied Mathematics (SIAM) Annual Meeting*, Pittsburgh, PA, July, 2017 (poster)
7. A.A. Mohekar, B.S. Tilley, and V.V. Yakovlev, Computational modelling of microwave heat exchangers, Soldier Science Research Symposium, Worcester Polytechnic Institute, Worcester, MA, February 2018.
8. J.M. Gaone, B.S. Tilley, and V.V. Yakovlev, Long-wave Homogenization of Porous Media Electromagnetic Heat Exchangers, *2018 MRS Spring Meeting*, Phoenix, AZ, April 2018.
9. A.A. Mohekar, B.S. Tilley, and V.V. Yakovlev, Computational modelling of triple layer EM heat exchangers, General Electric Research Center, Niskayuna, NY, April 2018.
10. A.A. Mohekar, Microwave heat exchangers, Massachusetts College of Liberal Arts (MCLA), North Adams, MA, April 2018. Invited Talk.
11. A.A. Mohekar, J.M. Gaone, V.V. Yakovlev, and B.S. Tilley, Electromagnetic Heat Exchangers in Energy Beaming Applications (Th3B), *IEEE MTT-S International Microwave Symposium, 3 Minute Thesis*, Philadelphia, PA. June 2018.
12. A.A. Mohekar, J.M. Gaone, B.S. Tilley, and V.V. Yakovlev, Multiphysics Simulation of Temperature Profiles in a Triple-Layer Model of a Microwave Heat Exchanger, *The 52nd Annual Microwave Power Symposium (IMPI 52)*, Long Beach, CA. June 2018.

13. J.M. Gaone, B.S. Tilley, V.V. Yakovlev, High-frequency Homogenization of Porous Media Electromagnetic Heat Exchangers, *SIAM Conference on Mathematical Aspects of Material Science*, Portland, OR, July 2018.
14. J.M. Gaone, B.S. Tilley, V.V. Yakovlev, High-frequency Homogenization of Porous Media Electromagnetic Heat Exchangers, *2018 MRS Fall Meeting*, Boston, MA. November 2018.
15. A.A. Mohekar, V.V. Yakovlev, B.S. Tilley, 2D numerical model of a triple layer EM heat exchangers, *2018 MRS Fall Meeting*, Boston, MA 2018. (poster)
16. J.M. Gaone, B.S. Tilley, V.V. Yakovlev, Long-wave homogenization of porous media electromagnetic heat exchangers, *International Mechanical Engineering Conference and Exposition*, Pittsburgh, PA. November 2018.
17. B.S. Tilley, J.M. Gaone, and V.V. Yakovlev, High-Frequency Homogenization of Porous Media Electromagnetic Heat Exchangers, *2019 MRS Spring Meeting*, Phoenix, AZ, April 2019.

Honors/Awards

1. Best Minisymposium Poster Award, A.A. Mohekar, 2D numerical model of a triple layer EM heat exchangers, Materials Research Society (MRS) Fall Meeting, Boston, MA 2018.